LA-UR-19-28727 (Accepted Manuscript)

Production of 230Pa by proton irradiation of 232Th at the LANL isotope production facility: Precursor of 230U for targeted alpha therapy

Friend, Mitchell Thomas
Mastren, Tara
Parker, Tracey Gannon
Vermeulen, Christiaan
Brugh, Mark
Birnbaum, Eva R.
Nortier, Francois Meiring
Fassbender, Michael Ernst

Provided by the author(s) and the Los Alamos National Laboratory (2019-11-07).

To be published in: Applied Radiation and Isotopes

DOI to publisher's version: 10.1016/j.apradiso.2019.108973

Permalink to record: http://permalink.lanl.gov/object/view?what=info:lanl-repo/lareport/LA-UR-19-28727

Disclaimer:
Los Alamos National Laboratory, an affirmative action/equal opportunity employer, is operated by Triad National Security, LLC for the National Nuclear Security Administration of U.S. Department of Energy under contract 89233218CNA000001. By approving this article, the publisher recognizes that the U.S. Government retains nonexclusive, royalty-free license to publish or reproduce the published form of this contribution, or to allow others to do so, for U.S. Government purposes. Los Alamos National Laboratory requests that the publisher identify this article as work performed under the auspices of the U.S. Department of Energy. Los Alamos National Laboratory strongly supports academic freedom and a researcher's right to publish; as an institution, however, the Laboratory does not endorse the viewpoint of a publication or guarantee its technical correctness.

Production of ^{230}Pa by Proton Irradiation of ^{232}Th at the LANL Isotope Production Facility: Precursor of ^{230}U for Targeted Alpha Therapy

Mitchell T. Friend[†], Tara Mastren[‡,†], T. Gannon Parker[†], Christiaan E. Vermeulen[†], Mark Brugh[†], Eva R. Birnbaum[†], F. Meiring Nortier[†] and Michael E. Fassbender[†,*]

[†]Chemistry Division, Los Alamos National Laboratory, P.O. Box 1663, Los Alamos, NM 87545, USA

[‡]Nuclear Engineering Program, Department of Civil and Environmental Engineering, University of Utah, 110 Central Campus Drive, Suite 2000b, Salt Lake City, UT 84112, USA

***Corresponding Author**
Michael E. Fassbender
Los Alamos National Laboratory MSJ975
Los Alamos, NM 87545
mifa@lanl.gov, radiochemistry@outlook.com
505-665-7306

Abstract

Uranium-230 ($t_{1/2}$ = 20.8 d) is an alpha-emitting radionuclide that has potential application in targeted alpha therapy (TAT) of cancer. Its parent isotope ^{230}Pa ($t_{1/2}$ = 17.4 d), can be produced by proton irradiation of thorium metal targets. Preliminary ^{230}Pa production runs were performed at the Los Alamos National Laboratory Isotope Production Facility (LANL-IPF) using thin thorium metal targets and a proton beam energy of 15-30 MeV, followed by radiochemical separation of ^{230}Pa from the irradiated target matrix. The measured ^{230}Pa production yields were found to exceed the predicted values in most of the experiments that were performed. This data will inform further production efforts for providing ^{230}Pa/^{230}U for clinical trials.

Keywords: Protactinium-230, Uranium-230, Thorium-226, Proton irradiation, Isotope production, Targeted alpha therapy

1. Introduction

Targeted alpha therapy (TAT) of cancer is a treatment method that utilizes the decay of an alpha-emitting radionuclide to apply a localized, cytotoxic dose of alpha radiation to tumor cells. The effectiveness of TAT lies in part in the physics of alpha-emission and translation of alpha-particles through matter. Alpha-particles typically have a path length <100 μm in biological material (a few cell diameters), and generate high ionization density along the flight path (i.e. the linear energy transfer (LET) of alpha-particles is high; on the order of 100 keV·μm^{-1}) (Kassis, 2008; Morgenstern et al., 2018). These properties make alpha-particles more effective at causing

double strand DNA damage, and therefore cell death, while minimizing radiation dose to surrounding healthy tissue when compared to beta-emitting radionuclides which have longer path lengths and lower LET (Morgenstern et al., 2018; Makvandi et al., 2018).

Therapeutic alpha-emitters need to have certain physical and nuclear properties in order to be potential candidates for TAT. Namely, they must have high branching ratios for alpha decay, short physical half-lives that produce acute doses of alpha radiation, and the ability to be attached to carrier biomolecules that deliver the radionuclide to the tumor site *in vivo*. Only a few alpha-emitters meet these criteria. A novel radionuclide for possible application in TAT is ^{230}U (Morgenstern et al., 2009). Uranium-230 ($t_{1/2}$ = 20.8 d) decays 100% by alpha-emission to a short-lived daughter; ^{226}Th ($t_{1/2}$ = 30.6 min). Thorium-226 also undergoes decay by alpha-emission, resulting in a decay cascade of four additional alpha-emissions (Fig. 1). The implication of the five successive alpha decays from each ^{230}U decay event is the culmination of an alpha dose in the range of 28-34 MeV that can be used in therapeutic applications. Uranium-230 may be used directly, or used to generate high specific activity ^{226}Th for TAT. Chelation of ^{227}Th ($t_{1/2}$ = 18.7 d) with conjugating molecules for TAT has already been demonstrated (^{226}Th and ^{227}Th differ in their nuclear properties, but have the same chemistry) (Ramdahl et al., 2016; Deblonde et al., 2018). However, production of ^{230}U/^{226}Th in relevant quantities is necessary for initiating clinical trials.

There are two primary pathways under consideration for producing ^{230}U. The first is by proton or deuteron bombardment of ^{231}Pa ($t_{1/2}$ = 32,760 y), which forms ^{230}U by the reactions ^{231}Pa(p,2n)^{230}U and ^{231}Pa(d,3n)^{230}U (Morgenstern et al., 2008a; Morgenstern et al., 2009). Protactium-231 is naturally occurring from the decay of ^{235}U ($t_{1/2} = 7.04 \times 10^8$ y, 0.72% abundance) in trace quantities. Higher quantities can be generated from primordial thorium (^{232}Th)

in a nuclear reactor via ^{232}Th(n,2n)^{231}Th → (β^--decay, 25.5 d) ^{231}Pa. Isolated ^{231}Pa and can then be made into targets by pressing into disks, or electrodepositing $^{231}Pa_2O_5$ onto a support material. Uranium-230 is produced directly from the nuclear reactions in this pathway. The other possible production pathway is by irradiating natural ^{232}Th ($t_{1/2} = 1.40 \times 10^{10}$ y) metal targets with protons or deuterons (Morgenstern et al., 2008b; Duchemin et al., 2014; Radchenko et al., 2016). Uranium-230 is made indirectly in this method by first producing ^{230}Pa through the reactions ^{232}Th(p,3n)^{230}Pa and ^{232}Th(d,4n)^{230}Pa, which then undergoes β^--decay to ^{230}U with a branching ratio of 7.8% and a 17.4 d half-life. Although indirect, the advantages of this production route are twofold: the thorium metal target material is generally more available than ^{231}Pa, and the ingrowth of ^{230}U from ^{230}Pa decay allows for the isolation of carrier-free ^{230}U without the presence of additional uranium isotopic impurities. The latter is desirable for eventual pharmaceutical manufacturing of a pure ^{230}U drug product. We have opted for the ^{232}Th(p,3n)^{230}Pa production route, followed by a radiochemical separation of ^{230}U from a ^{230}Pa/^{230}U generator system in the future. Preliminary proton irradiations of thorium metal targets need to be demonstrated, including radiochemical separation of the produced isotopes, in order to better understand the production capabilities and eventual yields of ^{230}Pa/^{230}U.

Herein, we report the results for preliminary ^{230}Pa production runs at the Los Alamos National Laboratory Isotope Production Facility (LANL-IPF) via proton irradiation of thorium metal targets. Irradiations were performed with thin targets at low beam current such that the resulting radioactivity of the irradiated targets was at a level that target processing could be performed in a radiological fume hood. Dissolution of the target and the separation of ^{230}Pa from the target matrix after irradiation was demonstrated using solid-phase extraction chromatography. This separation procedure was found necessary for reducing the background radiation signal for accurate

radiometric measurement of the ^{230}Pa production yield. Nickel foil monitor reactions were utilized to determine the proton beam energy, and simulations performed to predict the theoretical yield of ^{230}Pa which was compared to the experimental yield. Finally, the resulting ^{230}Pa production data obtained in this work was used in a modeling effort that described the anticipated production yields of ^{230}U in full scale production runs.

2. Experimental

2.1. Materials

All chemicals were reagent grade and used without further purification. Aqueous solutions were prepared with distilled, deionized water (18 MΩ·cm^{-1}, Millipore). Trace metal grade (Optima) nitric, hydrochloric, and hydrofluoric acids were purchased from Fisher Scientific (Pittsburgh, PA, USA). Chloride (CL) resin (100-150 µm particle size) was obtained from Triskem International (Bruz, France), and DGA resin (50-100 µm) from Eichrom Technologies (Lisle, IL, USA). Nickel monitor foils (99.999% purity) were acquired from Goodfellow USA (Coraopolis, PA, USA) that had thicknesses of 0.025 mm (tolerance <0.010 mm). Thorium targets were produced at the Los Alamos National Laboratory (LANL) using an internal inventory of thorium metal in the following manner: Pieces of thorium metal (>99% purity by X-ray fluorescence spectroscopy) were arc melted and rolled into sheets with a thickness of 0.50 ± 0.02 mm. Individual targets were cut from these sheets by electrical discharge machining, producing 1 g, 5.6 cm diameter targets with mass thicknesses of approximately 0.05 g·cm^{-2} (Fig. S1, Supplementary Information). Uncertainties in measured and calculated values presented throughout this work include propagated experimental error (e.g. target mass thickness and chemical yields from target dissolution and separation) and errors in the fitting parameters representing ±2σ.

2.2. Gamma-ray spectrometry

High purity germanium (HPGe) gamma-ray spectrometry measurements where performed using an EG&G Ortec Model GMX-35200-S HPGe combined with a Canberra Model 35-Plus multichannel analyzer. The detector contained a 0.5 mm beryllium window with outer dead layer thickness of 0.3 μm. Detector diameter was 50.0 mm and length 53.5 mm. System response was calibrated daily against a standard radionuclide mixture of ^{57}Co, ^{60}Co, ^{88}Y, ^{109}Cd, ^{113}Sn, ^{137}Cs, ^{139}Ce, ^{203}Hg and ^{241}Am, traceable to the National Institute of Standards and Technology (NIST) and supplied by Eckert & Ziegler (Atlanta, GA, USA). Uncertainties in the total source activities ranged from 2.6% to 3.3%. Counting dead time was kept below 10%. The characteristic gamma-rays used to identify ^{57}Co, ^{57}Ni and ^{230}Pa were taken from the National Nuclear Data Center (https://www.nndc.bnl.gov/nudat2/) and are shown in Table 1.

2.3. Proton irradiations

Thin thorium targets were irradiated for 30 min at LANL-IPF with an incident proton beam energy of 100.0 ± 0.1 MeV and a current of 10 μA. The beam current was measured non-destructively by an inductive current monitor upstream of the targets and fluctuated by 1% (±0.1 μA) throughout the irradiations. The targets were encased inside Inconel cladding and loaded in the LANL-IPF production stack "C-slot" position (Fig. S2, Supplementary Information). Aluminum energy degraders occupied slots "A" and "B" that attenuated the beam energy to 15-30 MeV. The targets were constructed to be larger than the beam size, which was collimated with an active four sector collimator. Beam was then tuned to fall inside the collimator. This ensured that the beam fell completely within the target area and left enough room around the edge to minimize the effect of scattering. The collimator aperture was 4.6 cm and the raster of the beam was adjusted to be slightly smaller. The beam energy that impinged on the thorium targets was

quantified by placing nickel energy monitor foils in front of the thorium targets and measuring the $^{57}Ni/^{57}Co$ activity ratio resulting from the reactions $^{nat}Ni(p,x)^{57}Ni$ and $^{nat}Ni(p,x)^{57}Co$ (Mastren et al., 2019). The targets were transported to the LANL radiochemistry facility for chemical processing and HPGe gamma-ray spectrometry analysis, typically within five days after end of bombardment (EOB).

2.4. Proton beam energy measurement with nickel monitor foils

The nickel monitor foils post irradiation were added to 10 mL of 10 M HNO_3 and heated to 150 °C to dissolve. The dissolved nickel foil was then evaporated to dryness, reconstituted in 5 mL of 10 M HNO_3 and transferred to a pre-weighed 20 mL scintillation vial. Dilutions of 1:5, 1:10, and 1:20 were prepared by weight after the mass of the dissolved nickel solution was determined, and then the activities of ^{57}Ni and ^{57}Co were measured via HPGe gamma-ray spectroscopy. The expected $^{57}Ni/^{57}Co$ activity ratio was calculated by:

$$\frac{A_1}{A_2} = \frac{\sigma_1\left(1 - e^{-\lambda_1 t_{irr}}\right)\left(e^{-\lambda_1 t_{EOB}}\right)}{\sigma_2\left(1 - e^{-\lambda_2 t_{irr}}\right)\left(e^{-\lambda_2 t_{EOB}}\right)} \quad (1)$$

where A_i is the activity of radionuclide i (Bq), σ_i is the production cross-section (cm^2), λ_i is the radioactive decay constant (s^{-1}), t_{irr} is the irradiation time (s), t_{EOB} is the time since EOB (s), and with $i = 1, 2$ corresponding to ^{57}Ni and ^{57}Co respectively. The effective cross-sections displayed in Table 2 for the reactions $^{nat}Ni(p,x)^{57}Ni$ and $^{nat}Ni(p,x)^{57}Co$ (cumulative; accounting for the decay of ^{57}Ni to ^{57}Co) were used to calculate the $^{57}Ni/^{57}Co$ activity ratio with Eq. (1) as a function of proton energies from 15 to 30 MeV. The average proton beam energy was determined from where the measured $^{57}Ni/^{57}Co$ activity ratios in the dissolved nickel monitor foils corresponded on the calculated $^{57}Ni/^{57}Co$ verses proton energy curve (Fig. S3, Supplementary Information).

2.5. Thorium target dissolution and ^{230}Pa measurement

The irradiated thorium targets were removed from the Inconel cladding and dissolved in a Teflon beaker under gentle heating with 40 mL of 10 M HCl/0.01 M HF. Protactinium-230 was separated from bulk thorium and fission products using the methodology described in a previous work (Mastren et al., 2018). Specifically, a 1 mL CL resin column (0.35 g dry resin) was prepared in a 10 mL BioRad poly prep column, washed with three bed volumes of water and then equilibrated with three bed volumes of 10 M HCl. The dissolved target was loaded onto the column and then washed with 20 mL of 10 M HCl to remove bulk thorium and fission products. Protactinium-230 and remaining ^{95}Nb were stripped from the CL column with 10 mL of 4 M HCl/0.1 M HF, evaporated to dryness, and dissolved in 10 mL of 10 M HNO_3. This solution was then loaded onto a 1 mL DGA resin column (0.4 g dry resin) that was previously conditioned with three bed volumes of water followed by three bed volumes of 10 M HNO_3. Niobium-95 was removed with 20 mL of 1 M HNO_3, and then ^{230}Pa was eluted with 10 mL of 4 M HCl/0.1 M HF. The activity of ^{230}Pa was determined with HPGe gamma-ray spectroscopy from dilutions of 1:5, 1:10, and 1:20 by weight, and then its production yield calculated in MBq per μAh of irradiation.

2.6. Calculation of ^{230}Pa production yield

The activity of a radionuclide produced by a charged particle irradiation of a target material is calculated by:

$$A_{\mathrm{EOB}} = \frac{dN_{\mathrm{A}}\sigma I}{Mze}\left(1 - \mathrm{e}^{-\lambda t_{\mathrm{irr}}}\right) \tag{2}$$

where A_{EOB} is the activity of the produced radionuclide at EOB (Bq), d is the mass thickness of the target (g·cm^{-2}), N_{A} is Avogadro's number (6.02214×10^{23} mol^{-1}), σ is the production cross-section for the produced radionuclide at a given beam energy (cm^2), I is the beam current (A), M is the molar mass of the target atoms (g·mol^{-1}), z is the charge of the particle beam ($z = 1$ for protons), e is the elementary charge (1.602177×10^{-19} C), λ is the radioactive

decay constant of the produced radionuclide (s^{-1}), and t_{irr} is the irradiation time (s). Measured activities, A (Bq), of produced radionuclides were corrected to EOB by:

$$A = A_{EOB} e^{-\lambda t_{EOB}} \quad (3)$$

where t_{EOB} is the time that has passed since EOB (s).

A Stopping and Range of Ions in Matter (SRIM) simulation was used to model the proton beam energy distribution that penetrated the thin thorium targets (Ziegler et al., 2010). The model simulated the transmission of 10,000 ions through the material upstream of the thorium target using the average incident energy measured from the nickel monitor foil reactions as described in Section 2.4. The ions were binned in 0.5 MeV intervals and normalized to unity, i.e. the sum of the population across all the bins equaled one. An example is plotted in Fig. 2 and was fit by a Gaussian distribution. The proton current transmitted through the thorium target also was scaled to the number of normalized ions across the energy distribution determined by the Gaussian fit.

Excitation functions for the ^{232}Th(p,3n)^{230}Pa reaction in the range of 10-30 MeV were collected from the Experimental Nuclear Reaction Database (https://www-nds.iaea.org/exfor/exfor.htm; Celler et al., 1981; Kudo et al., 1982; Morgenstern et al., 2008b; Jost et al., 2013). This data was plotted in Fig. 3 and fit with a sixth order polynomial. The production cross-section at each proton energy was calculated from the polynomial fit equation and tabulated in Table 2. The theoretical activity of ^{230}Pa produced at EOB was calculated with Eq. (2), using the scaled values of the proton current and cross-section for all the proton energies in the SRIM energy distribution. These activities were then summed to give the total theoretical activity of ^{230}Pa produced in each irradiation, and then compared to the experimentally measured ^{230}Pa activity.

3. Results and discussion

3.1. ^{230}Pa production yields

Three separate irradiations were performed over the course of a year. Measurement of the ^{57}Ni/^{57}Co activity ratios in the nickel monitor foils indicated that the average proton beam energies that interacted with the thin thorium targets were 19 ± 1 MeV (January 2017), 24 ± 1 MeV (September 2017), and 27 ± 1 MeV (January 2018). These energies were used in the SRIM simulations which predicted the loss of 0.19% protons due to scatter, and a lateral range through the incident on the thorium targets with a mean absolute value of ~6 mm. Uncertainties in the production yield calculations were conservatively increased by 10% to account for potential loss of proton fluence due to nuclear reactions in the aluminum degraders.

Protactinium-230 was isolated from the bulk thorium target matrix, activation products, and fission products using CL and DGA extraction chromatography resins with a chemical yield of 93 ± 4%. Radiochemical purity of protactinium radionuclides was >99%—^{229}Pa and ^{231}Pa from the ^{232}Th(p,4n)^{229}Pa and ^{232}Th(p,2n)^{231}Pa reactions were co-produced with ^{230}Pa, but represented <0.1% of total protactinium by activity percent at the time of chemical processing (five to ten days after EOB)—with the presence of <0.5% of ^{95}Nb as the remaining radionuclide contaminant. This radiochemical purity is satisfactory for use as parent material for generating carrier free ^{230}U for TAT. Moreover, separation of ingrown ^{230}U from the ^{230}Pa/^{230}U generator using an additional DGA column would entail the removal of residual ^{95}Nb contaminant (Pourmand and Dauphas, 2010; Mastren et al., 2018).

Table 3 compares the predicted ^{230}Pa production yields with the experimentally determined yields from the three irradiations. The first irradiation under-produced ^{230}Pa with a yield of 88 ± 7% of the theoretically predicted amount. The irradiations that followed appeared to overproduce ^{230}Pa however, with yields of 118 ± 9% and 110 ± 8% respectively. This discrepancy

in yield highlights a need for additional cross section measurements for the ^{232}Th(p,3n)^{230}Pa reaction. However, the measured production yields are still within 10% error of the theoretical yields.

3.2. Projected yields of ^{230}U for TAT

The data collected from these irradiation experiments were used to estimate the amount of ^{230}U that could be made available for TAT in a full scale production run. Figure 4 shows the projected production of ^{230}Pa and ^{230}U after a two day irradiation using the irradiation parameters from the September 2017 irradiation listed in Table 3. Over the course of a two day irradiation the SRIM predicted production rate of ^{230}Pa (0.31 ± 0.01 MBq·μAh^{-1}) indicates that 2.9 GBq (79 mCi) of ^{230}Pa could be produced at EOB. Similarly, the experimental measured production rate of 0.37 ± 0.03 MBq·μAh^{-1} predicts the generation of 3.5 GBq (95 mCi) of ^{230}Pa at EOB. The decay of ^{230}Pa to ^{230}U over a period of 28 d after EOB gave projected yields of 0.17 GBq (4.5 mCi) and 0.20 GBq (5.4 mCi) of ^{230}U, using the predicted and experimental production yields respectively.

The same modeling exercise was performed simulating a two day irradiation of a thick thorium target having a mass thickness of 0.5 g·cm^{-2}, with beam energies between 20 and 30 MeV and at a current of 250 μA (Fig. S4, Supplementary Information). These conditions are indicative of a full scale production run that could be performed at LANL-IPF. Projected ^{230}Pa yields of 11-57 GBq (0.31-1.5 Ci) at EOB could be expected under these irradiation conditions, and implies that up to 3.2 GBq (87 mCi) of ^{230}U would be able to be separated 28 d after EOB. The production cross-sections for the alternative ^{231}Pa(p,2n)^{230}U pathway are an order of magnitude lower (max cross-section 33 ± 5 mb at 14.6 MeV) than for ^{232}Th(p,3n)^{230}Pa, and as a result the yields of ^{230}U are comparable between the two production methods despite the 7.8% branching ratio for the decay of ^{230}Pa to ^{230}U (Morgenstern et al., 2008a). Additionally, the deuteron induced nuclear reactions

have predicted production yields that are less than the corresponding proton induced nuclear reactions (Duchemin et al., 2014). The relative ease of obtaining and handling quasi-stable ^{232}Th versus radioactive ^{231}Pa for targetry makes the indirect ^{232}Th(p,3n)^{230}Pa → (β^--decay) ^{230}U route the preferred method without a significant advantage in ^{230}U production yield for the ^{231}Pa reactions. Moreover, ^{230}U can continually be separated from ^{230}Pa that was isolated in previous production campaigns as it continues to decay to ^{230}U, providing an ongoing supply of ^{230}U for TAT.

Actinium-225 ($t_{1/2}$ = 9.92) is another important alpha-emitter for TAT, and is produced in clinically relevant quantities by irradiating ^{232}Th with high energy (≥100 MeV) protons. Predicted thick target yields of ^{225}Ac have been reported as 52 GBq (100 MeV, 250 μA) to 74 GBq (200 MeV, 100 μA) after ten day irradiations (Weidner et al., 2012). The ^{225}Ac yields are an order of magnitude greater than what we have predicted is achievable for ^{230}U, although the co-production of approximately 0.1% by activity of the long-lived and undesired ^{227}Ac ($t_{1/2}$ = 21.8 y) isotope is a challenge associated with accelerator production of ^{225}Ac. The ^{230}U/^{226}Th system could serve as a compliment to ^{225}Ac for TAT, where routine production of ^{230}Pa/^{230}U would be suitable at low energy cyclotrons that are not able to achieve the high proton energies required for bulk production of ^{225}Ac. Actinium-225 and ^{230}Pa/^{230}U could be produced simultaneously at LANL-IPF however, with ^{225}Ac production occurring in the high energy "A-slot" (100 MeV incident energy) and ^{230}Pa/^{230}U production in the low energy "C-slot" (35 MeV incident energy). Targeted alpha therapy treatments that used three cycles of ~10 MBq of ^{225}Ac (generally 100 kBq per kg of body weight) have shown exceptional results in the treatment of metastasized castration-resistant prostate cancer (Kratochwil et al., 2016). Our results indicate

that LANL-IPF could produce enough ^{230}U to treat on the order of 100 patients after a full production run, assuming a similar dose of $^{230}U/^{226}Th$ and treatment cycle would be applied.

4. Conclusion

Protactinium-230 was produced from the irradiation of thin thorium targets with 15-30 MeV protons. Nickel energy monitor foils were used to determine the average proton energy transmitting though the thorium targets, and a SRIM model applied to describe the energy distribution. The separation of ^{230}Pa from the bulk thorium and fission products in irradiated target material was accomplished with high chemical yield and radiochemical purity. This also reduced the counting background and dead time, providing for accurate radiometric determination of the ^{230}Pa production yield. A combination of these measurements and models were used to project to scaled up production yields, demonstrating the feasibility of the $^{232}Th(p,3n)^{230}Pa$ production pathway for the indirect production of ^{230}U for TAT. Future production runs will utilize thick targets and full beam power necessitating the use of a hot cell facility. Thick target ^{230}Pa yields will be measured and a $^{230}Pa/^{230}U$ generator deployed to provide usable quantities of ^{230}U for bioconjugation experiments.

Acknowledgments

This research was supported by the U.S. Department of Energy Isotope Program, managed by the Office of Science for Nuclear Physics (grant awarded under FOA LAB 14-1099). We thank the staff of the C-IIAC, LANSCE-AOT, and Sigma-1 groups at the Los Alamos National Laboratory for assistance with experiments.

Appendix A. Supplementary Information

References

Celler, A., Luontama, M., Kantele, J., 1981. Cross Sections of ^{232}Th(p,xn+yp) Reactions at E_p = 6.8 to 20.2 MeV. Physica Scripta 24, 930-934.

Deblonde, G.J.-P., Lohrey, T.D., Booth, C.H., Carter, K.P., Parker, B.F., Larsen, Å., Smeets, R., Ryan, O.B., Cuthbertson, A.S., Abergel, R.J., 2018. Solution Thermodynamics and Kinetics of Metal Complexation with a Hydroxypyridinone Chelator Designed for Thorium-227 Targeted Alpha Therapy. Inorg. Chem. 57 (22), 14337-14346.

Duchemin, C., Guertin, A., Haddad, F., Michel, N., Métivier, V., 2014. ^{232}Th(d,4n)^{230}Pa cross-section measurements at ARRONAX facility for the production of ^{230}U. Nucl. Med. Biol. 41, e19-e22.

Jost, C.U., Griswold, J.R., Bruffey, S.H., Mirzadeh, S., Stracener, D.W., Williams, C.L., 2013. Measurement Of Cross Sections For The ^{232}Th (P, 4n) ^{229}Pa Reaction At Low Proton Energies. AIP Conf. Proc. 1525, 520-524.

Kassis, A.I., 2008. Therapeutic Radionuclides: Biophysical and Radiobiologic Principles. Semin. Nucl. Med. 38 (5), 358-366.

Kratochwil, C., Bruchertseifer, F., Giesel, F.L., Weis, M., Verburg, F.A., Mottaghy, F., Kopka, K., Apostolidis, C., Haberkorn, U., Morgenstern, A., 2016. ^{225}Ac-PSMA-617 for PSMA-Targeted α-Radiation Therapy of Metastatic Castration-Resistant Prostate Cancer. J. Nucl. Med. 57 (12), 1941-1944.

Kudo, H., Muramatsu, H., Nakahara, H., 1982. Fission fragment yields in the fission of ^{232}Th by protons of energies 8 to 22 MeV. Phys. Rev. C 25 (6) 3011-3023.

Makvandi, M., Dupis, E., Engle, J.W., Nortier, F.M., Fassbender, M.E., Simon, S., Birnbaum, E.R., Atcher, R.W., John, K.D., Rixe, O., Norenberg, J.P., 2018. Alpha-Emitters and Targeted Alpha Therapy in Oncology: from Basic Science to Clinical Investigations. Targeted Oncol. 13, 189-203.

Mastren, T., Stein, B.W., Parker, T.G., Radchenko, V., Copping, R., Owens, A., Wyant, L.E., Brugh, M., Kozimor, S.A., Nortier, F.M., Birnbaum, E.R., John, K.D., Fassbender, M.E., 2018. Separation of Protactinium Employing Sulfur-Based Extraction Chromatographic Resins. Anal. Chem. 90, 7012-7017.

Mastren, T., Vermeulen, C., Brugh, M., Birnbaum, E.R., Nortier, M.F., Fassbender, M.E., 2019. Natural nickel as a proton beam energy monitor for energies ranging from 15 to 30 MeV. Nucl. Instrum. Meth. B 443, 1-4.

Morgenstern, A., Lebeda, O., Stursa, J., Bruchertseifer, F., Capote, R., McGinley, J., Rasmussen, G., Sin, M., Zielinska, B., Apostolidis, C., 2008a. Production of ^{230}U/^{226}Th for Targeted Alpha Therapy via Proton Irradiation of ^{231}Pa. Anal. Chem. 80 (22), 8763-8770.

Morgenstern, A., Apostolidis, C., Bruchertseifer, F., Capote, R., Gouder, T., Simonelli, F., Sin, M., Abbas, K., 2008b. Cross-sections of the reaction ^{232}Th(p,3n)^{230}Pa for production of ^{230}U for targeted alpha therapy. Appl. Radiat. Isot. 66, 1275-1280.

Morgenstern, A., Lebeda, O., Stursa, J., Capote, R., Sin, M., Bruchertseifer, F., Zeilinska, B., Apostolidis, C., 2009. Cross sections of the reaction ^{231}Pa(d,3n)^{230}U for the production of ^{230}U/^{226}Th for targeted α therapy. Phys. Rev. C 80 (5), 054612.

Morgenstern, A., Apostolidis, C., Kratochwil, C., Sathekge, M., Krolicki, L., Bruchertseifer, F., 2018. An Overview of Targeted Alpha Therapy with ^{225}Actinium and ^{213}Bismuth. Curr. Radiopharm. 11 (3), 200-208.

National Nuclear Data Center, Chart of Nuclides, Brookhaven National Laboratory. https://www.nndc.bnl.gov/nudat2/.

National Nuclear Data Center, Experimental Nuclear Reaction Database, Brookhaven National Laboratory, 1994, v2018-04-25. https://www-nds.iaea.org/exfor/exfor.htm.

Pourmand, A., Dauphas, N., 2010. Distribution coefficients of 60 elements on TODGA resin: Application to Ca, Lu, Hf, U, and Th isotope geochemistry. Talanta 81 (3), 741-753.

Radchenko, V., Engle, J.W., Wilson, J.J., Maassen, J.R., Nortier, M.F., Birnbaum, E.R., John, K.D., Fassbender, M.E., 2016. Formation cross-sections and chromatographic separation of protactinium isotopes formed in proton-irradiated thorium metal. Radichim. Acta 104 (5), 291-304.

Ramdahl, T., Bonge-Hansen, H.T., Ryan, O.B., Larsen, Å., Herstad, G., Sandberg, M., Bjerke, R.M., Grant, D., Brevik, E.M., Cuthbertson, A.S., 2016. An efficient chelator for complexation of thorium-227. Bioorg. Med. Chem. Lett. 26, 4318-4321.

Weidner, J.W., Mashnik, S.G. John, K.D., Hemez, F., Ballard, B., Bach, H., Birnbaum, E.R., Bitteker, L.J., Couture, A., Dry, D., Fassbender, M.E., Gulley, M.S., Jackman, K.R., Ullmann, J.L., Wolfsberg, L.E., Nortier, F.M., 2012. Proton-induced cross sections relevant to production of ^{225}Ac and ^{223}Ra in natural thorium targets below 200 MeV. Appl. Radiat. Isot. 70, 2606-2607.

Ziegler, J.F., Ziegler, M.D., Biersack, J.P., 2010. SRIM - The stopping and range of ions in matter (2010). Nucl. Instrum. Meth. B 268, 1818-1823.

List of Figures

Fig. 1. Decay scheme of ^{230}Pa/^{230}U/^{226}Th. The successive five alpha decays of ^{230}U/^{226}Th delivers a total alpha dose of approximately 28-34 MeV making the isotopes desirable for TAT of cancer.

Fig. 2. SRIM simulation of the proton energy distribution through the thorium target. The experimental average proton energy of 24 ± 1 MeV, determined from the ^{57}Ni/^{57}Co activity ratio measured in the nickel monitor foil, was used in this example. Ten thousand simulated ions were binned in 0.5 MeV intervals and fit with a Gaussian distribution with $\mu = 23.83 \pm 0.06$ MeV, $\sigma = 2.17 \pm 0.08$ MeV, FWHM = 5.1 ± 0.2 MeV at 95% confidence.

Fig. 3. Excitation functions and the corresponding fit for the reaction ^{232}Th(p,3n)^{230}Pa.

Fig. 4. Modeled thin target production of ^{230}Pa from the reaction ^{232}Th(p,3n)^{230}Pa with a 24 ± 1 MeV proton beam using the theoretically predicted (red and green traces) production rate of 0.31 ± 0.01 MBq·μAh^{-1} of ^{230}Pa, and the experimentally determined (black and blue traces) production rate of 0.37 ± 0.03 MBq·μAh^{-1} of ^{230}Pa. Solid traces represent the calculated values and the dashed traces represent a 95% confidence band. A two day irradiation was simulated showing the decay of ^{230}Pa and ingrowth of ^{230}U occurring for 28 d after EOB (represented by the vertical line).

List of Tables

Table 1. Principal gamma-ray emissions of radionuclides measured in this work from the National Nuclear Data Center (https://www.nndc.bnl.gov/nudat2/).

Table 2. Effective cross-sections for the $^{nat}Ni(p,x)^{57}Ni$, $^{nat}Ni(p,x)^{57}Co$ (cumulative) and $^{232}Th(p,3n)^{230}Pa$ reactions for proton energies ranging from 15 to 30 MeV.

Table 3. Production rates of ^{230}Pa from proton irradiated thin thorium targets.

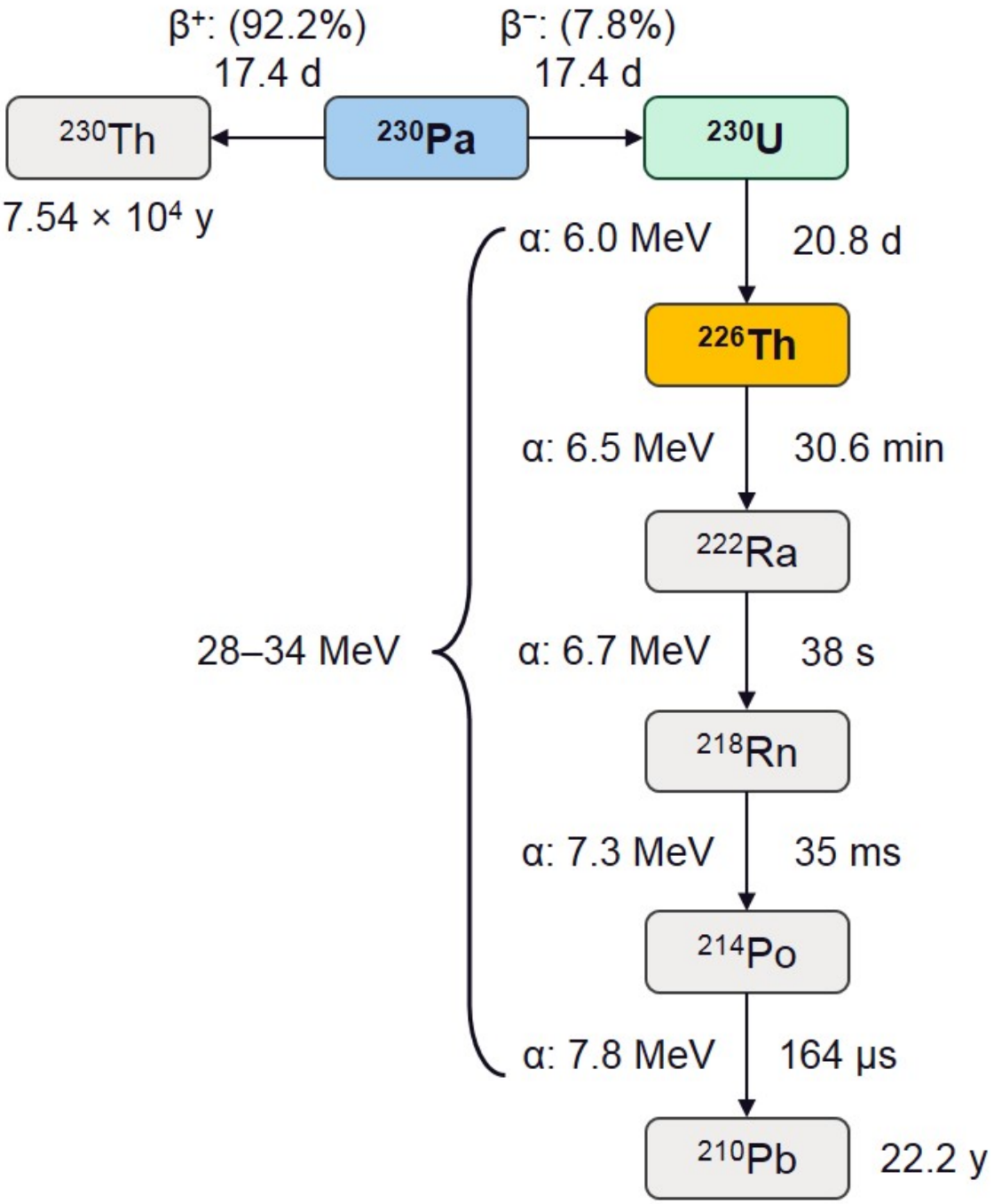

Fig. 1. Decay scheme of ^{230}Pa/^{230}U/^{226}Th. The successive five alpha decays of ^{230}U/^{226}Th delivers a total alpha dose of approximately 28-34 MeV making the isotopes desirable for TAT of cancer.

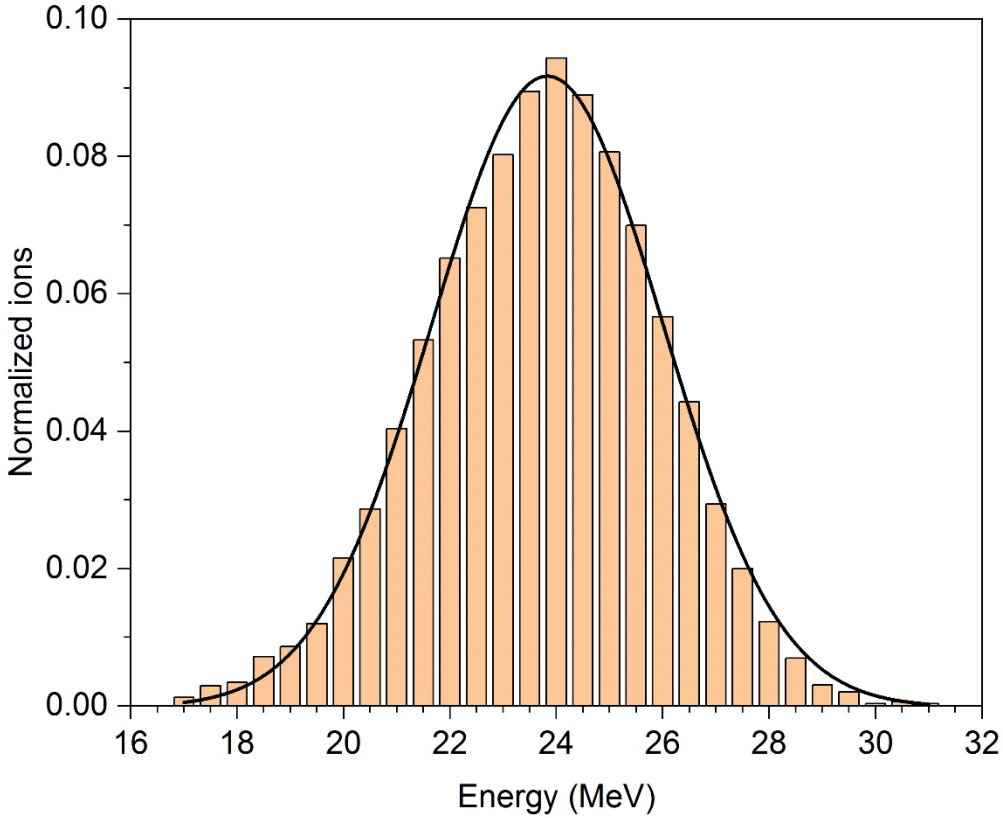

Fig. 2. SRIM simulation of the proton energy distribution through the thorium target. The experimental average proton energy of 24 ± 1 MeV, determined from the $^{57}Ni/^{57}Co$ activity ratio measured in the nickel monitor foil, was used in this example. Ten thousand simulated ions were binned in 0.5 MeV intervals and fit with a Gaussian distribution with $\mu = 23.83 \pm 0.06$ MeV, $\sigma = 2.17 \pm 0.08$ MeV, FWHM = 5.1 ± 0.2 MeV at 95% confidence.

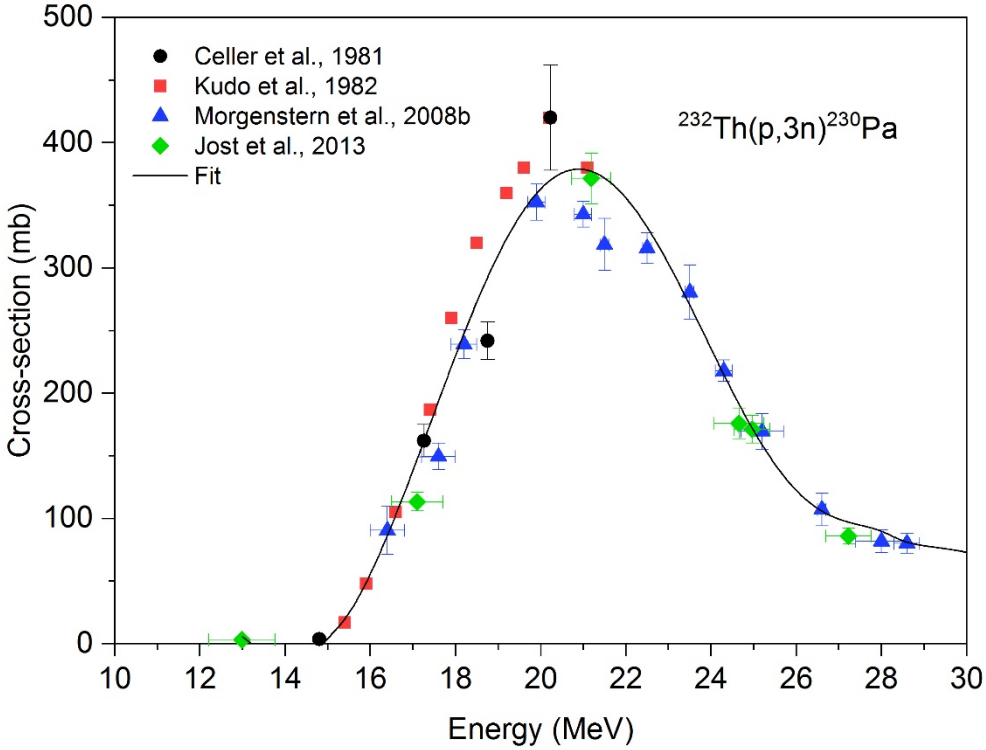

Fig. 3. Excitation functions and the corresponding fit for the reaction ^{232}Th(p,3n)^{230}Pa.

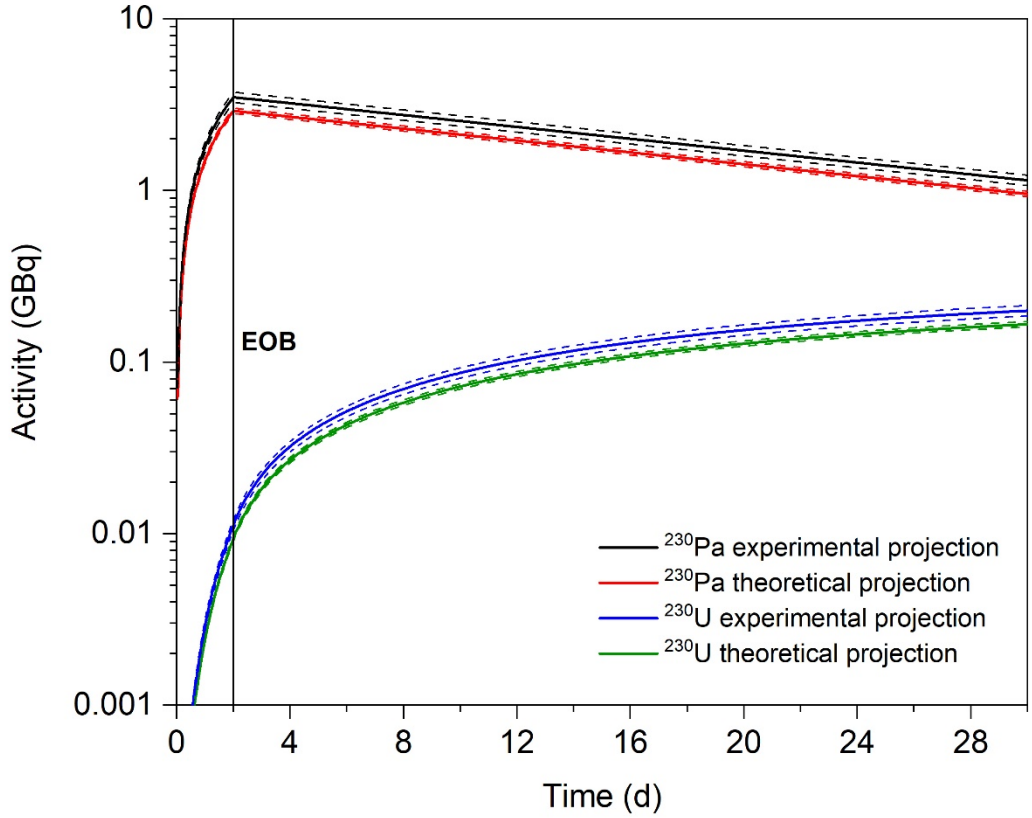

Fig. 4. Modeled thin target production of ^{230}Pa from the reaction ^{232}Th(p,3n)^{230}Pa with a 24 ± 1 MeV proton beam using the theoretically predicted (red and green traces) production rate of 0.31 ± 0.01 MBq·μAh^{-1} of ^{230}Pa, and the experimentally determined (black and blue traces) production rate of 0.37 ± 0.03 MBq·μAh^{-1} of ^{230}Pa. Solid traces represent the calculated values and the dashed traces represent a 95% confidence band. A two day irradiation was simulated showing the decay of ^{230}Pa and ingrowth of ^{230}U occurring for 28 d after EOB (represented by the vertical line).

Table 1

Principal gamma-ray emissions of radionuclides measured in this work from the National Nuclear Data Center (https://www.nndc.bnl.gov/nudat2/).

Radionuclide	Half-life	Gamma-ray energy (keV)	Branching ratio (%)
^{57}Co	271.74 d	122.06	85.6
		136.47	10.7
^{57}Ni	35.60 h	127.16	16.7
		1377.63	81.7
^{230}Pa	17.4 d	454.92	6.8
		918.50	8.3
		951.88	29.6

Table 2

Effective cross-sections for the $^{nat}Ni(p,x)^{57}Ni$, $^{nat}Ni(p,x)^{57}Co$ (cumulative) and $^{232}Th(p,3n)^{230}Pa$ reactions for proton energies ranging from 15 to 30 MeV.

Energy (MeV)	$^{nat}Ni(p,x)^{57}Ni$ (mb)[a]	$^{nat}Ni(p,x)^{57}Co$ (mb)[a]	$^{232}Th(p,3n)^{230}Pa$ (mb)[b]
15	10	188	4
15.5	18	235	23
16	26	280	55
16.5	36	322	94
17	46	362	138
17.5	57	398	185
18	68	430	231
18.5	79	459	274
19	90	484	312
19.5	100	505	343
20	111	523	365
20.5	121	537	377
21	130	548	380
21.5	138	555	373
22	146	560	357
22.5	153	561	334
23	159	560	304
23.5	164	557	271
24	168	552	235
24.5	171	545	201
25	174	536	169
25.5	175	526	142
26	175	515	121
26.5	175	503	107
27	173	490	99
27.5	171	477	95
28	168	463	91
28.5	165	449	81
29	161	435	78
29.5	157	420	76
30	152	406	73

[a]From (Mastren et al., 2019).

[b]Calculated from the sixth order polynomial fit in Fig. 3.

Table 3

Production rates of ^{230}Pa from proton irradiated thin thorium targets.

Date of irradiation	Average beam energy (MeV)[a]	Th target mass thickness (g·cm^{-2})	Predicted ^{230}Pa production rate (MBq·μAh^{-1})[b]	Measured ^{230}Pa production rate (MBq·μAh^{-1})[b]	^{230}Pa yield (% of theoretical)
January 2017	19 ± 1	0.0452 ± 0.001	0.31 ± 0.01 (8.3 ± 0.3)	0.27 ± 0.02 (7.3 ± 0.5)	88 ± 7
September 2017	24 ± 1	0.0452 ± 0.001	0.31 ± 0.01 (8.5 ± 0.3)	0.37 ± 0.03 (10.1 ± 0.7)	118 ± 9
January 2018	27 ± 1	0.0484 ± 0.001	0.20 ± 0.01 (5.3 ± 0.3)	0.22 ± 0.01 (5.9 ± 0.4)	110 ± 9

[a]Measured by nickel energy monitor foils.

[b]Values in parentheses given in μCi·μAh^{-1}.

[c]Uncertainties reported as ±2σ.